


# Postharvest Ultrasound-Assisted Freeze-Thaw Pretreatment Improves the Drying Efficiency, Physicochemical Properties, and Macamide Biosynthesis of Maca (*Lepidium meyenii*)

Jin-Jin Chen , Peng-Fei Gong, Yi-Lan Liu, Bo-Yan Liu, Dawn Eggert, Yuan-Heng Guo, Ming-Xia Zhao, Qing-Sheng Zhao, and Bing Zhao

**Abstract:** A novel technique of ultrasound-assisted freeze-thaw pretreatment (UFP) was developed to improve the drying efficiency of maca and bioactive amide synthesis in maca. The optimal UFP conditions are ultrasonic processing 90 min at 30 °C with 6 freeze-thaw cycles. Samples with freeze-thaw pretreatment (FP), ultrasound pretreatment (UP), and UFP were prepared for further comparative study. A no pretreatment (NP) sample was included as a control. The results showed that UFP improved the drying efficiency of maca slices, showing the highest effective moisture diffusivity ( $1.75 \times 10^{-9} \text{ m}^2/\text{s}$ ). This result was further supported by low-field nuclear magnetic resonance (LF-NMR) analysis and scanning electron microscopy (SEM). The rehydration capacity and protein content of maca slices were improved by UFP. More importantly, contents of bioactive macamides and their biosynthetic precursors were increased in 2.5- and 10-fold, respectively. In conclusion, UFP is an efficient technique to improve drying efficiency, physicochemical properties, and bioactive macamides of maca, which can be applied in the industrial manufacture of maca products.

**Keywords:** drying efficiency, *Lepidium meyenii*, macamides biosynthesis, physicochemical properties, ultrasound-assisted freeze-thaw pretreatment

## Introduction

The root of *Lepidium meyenii* Walp. (maca) has been used as both a dietary staple and a traditional medicine in the Andes for centuries (Gonzales, 2012). Macamides are the major active ingredients of maca, which play a stimulatory role in the central nervous system, showing positive effects for neuroprotection and prevention of osteoporosis (Almukadi et al., 2013; Alquraini, Wag-gas, Böhlke, Maher, & Pino-Figueroa, 2014; Hajdu et al., 2014; Lewis & Pino-Figueroa, 2013; Liu et al., 2015; Wu, Kelley, Pino-Figueroa, Vu, & Maher, 2013).

Macamides are absent from fresh maca roots but are formed during postharvest drying. The putative biosynthetic pathway of macamide is shown in Figure 1 (Chen et al., 2017; Esparza, Hadzich, Kofer, Mithöfer, & Cosio, 2015). Glucosinolates are hydrolyzed by myrosinase to benzyl isothiocyanate and converted to benzylamine (a). Membrane and storage lipids are hydrolyzed into free fatty acids (b). Macamides are formed by 1 benzylamine and 1 fatty acid moiety (c). However, in intact cells, glucosinolates and myrosinase (EC 3.2.3.1) are in different compartments, and free fatty acids exist in the form of lipids (Bones & Rossiter, 1996;

Dussert et al., 2006). Cell damage during postharvest process is beneficial for glucosinolate breakdown as it accelerates the release of free fatty acids (Dussert et al., 2006; Yábar, Pedreschi, Chirinos, & Campos, 2011). Commonly used methods for maca postharvest processing are the traditional open-field and industrial oven drying. Traditional open-field drying takes approximately 90 d in extreme temperature conditions ranging from -10 °C to 15 °C and is vulnerable to frost and other weather effects (Yábar et al., 2011). Industrial oven drying (always >50 °C) seriously inhibits the biosynthesis of macamides (Chen et al., 2017; Pan, Zhang, Li, Wang, & Li, 2016). Therefore, an effective method for maca postharvest processing is needed.

Freeze-thaw treatment has been reported to be a useful method to increase the drying rate of several agricultural products. Zhang and Willison (1992) proved freeze-thaw cycling injured the plasma membrane and tonoplast of potato and carrot tissues using electrical impedance analysis. Vaccarezza, Lombardi, and Chirife (1974) and Ando et al. (2016) suggested the modification of permeability of plant tissues and the formation of ice crystals facilitated water migration. Ultrasound has attracted considerable interests as a food processing technology in recent years. Heating effects, cavitation phenomenon and structural effects are among some of the proposed mechanisms of action for ultrasound (Jambrak, Mason, Paniwnyk, & Lelas, 2007). These effects help to disintegrate or damage the cell membranes, walls or tissues. Due to these effects, the heat and mass transfer rates between the cell and its extracellular surroundings are highly increased. Therefore, ultrasound has been widely used to assist freezing, blanching, drying and sterilization in the food technology applications of processing, preservation and extraction (Chemat & Khan, 2011).

In this study, a novel technique of ultrasound-assisted freeze-thaw pretreatment (UFP) was designed to improve drying

JFDS-2017-1559 Submitted 9/20/2017, Accepted 1/23/2018. Authors Chen, Gong, B.-Y. Liu, Guo, M.-X. Zhao, Q.-S. Zhao and B. Zhao are with State Key Laboratory of Biochemical Engineering, Inst. of Process Engineering, Chinese Acad. of Sciences, Beijing 100190, China. Authors Chen and Eggert are with Dept. of Food Science and Technology, Univ. of Nebraska-Lincoln, Lincoln, N.E. 68588, U.S.A. Author Y.-L. Liu is with Dept. of Chemical and Biomolecular Engineering, Univ. of Nebraska-Lincoln, Lincoln, N.E. 68588, U.S.A. Authors Gong, B.-Y. Liu and Guo are also with Univ. of Chinese Acad. of Sciences, Beijing 100049, China. Direct inquiries to authors Q.-S. Zhao and B. Zhao (E-mail: qszhao@ipe.ac.cn, bzhaob@ipe.ac.cn).

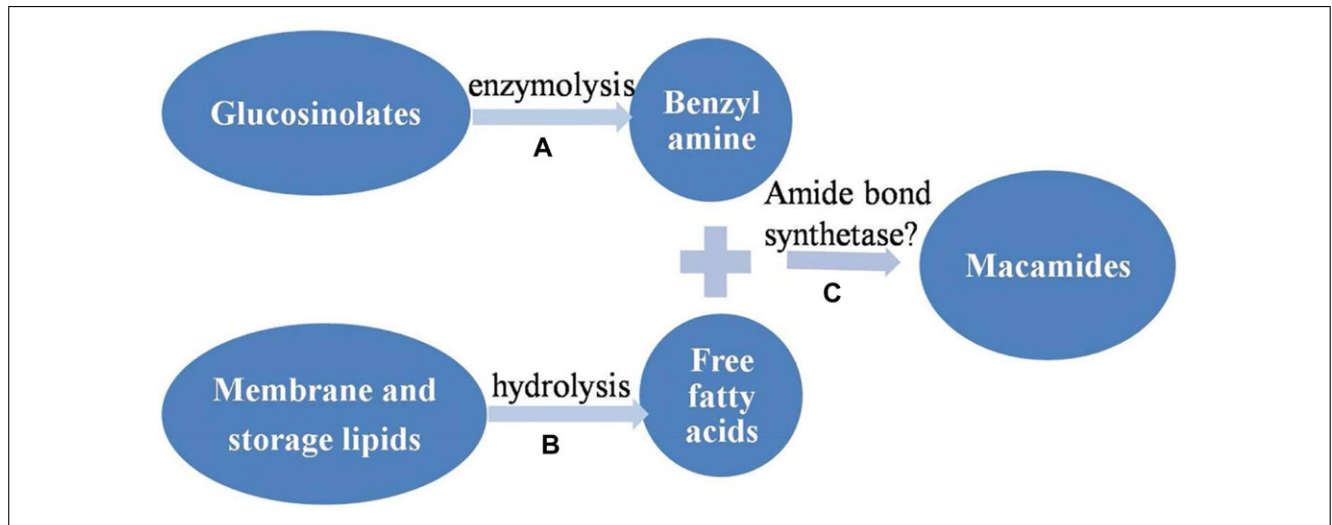


Figure 1–Biosynthesis pathway of macamides.

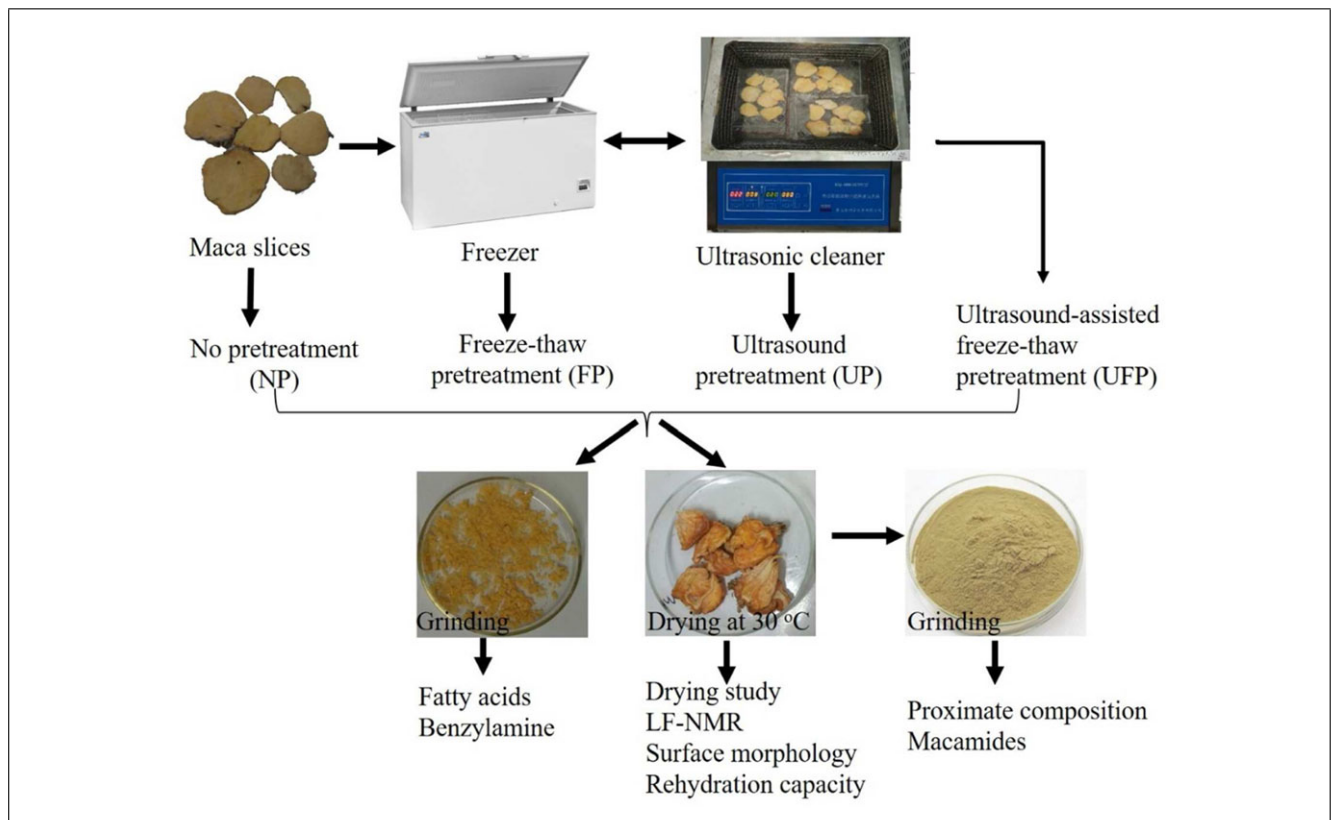


Figure 2–The experimental design of this study.

efficiency, physicochemical properties and macamide biosynthesis of maca. First, the parameters for UFP were optimized, then comparisons among samples of no pretreatment (NP), freeze-thaw pretreatment (FP), ultrasound pretreatment (UP), and UFP were carried out. Figure 2 shows the experimental design.

## Materials and Methods

### Chemicals and plant materials

Benzylamine, linolenic and linoleic acids were purchased from Sigma Chemical Co. (St. Louis, MO, U.S.A.). Three main

macamide reference substances, including *N*-benzyl-9Z, 12Z, 15Z-octadecatrienamide, *N*-benzyl-9Z, 12Z-octadecadienamide and *N*-benzyl-hexadecanamide, were synthesized by our laboratory (Figure S1). Acetonitrile, methanol, formic acid and water are HPLC grade. Other chemicals used were of analytical grade.

Fresh yellow maca were obtained from Wenbi mountain of Lijiang, Southwest China (100°25'E, 26°86'N) at 3200 m altitude in January 2016. Samples were evenly cut into slices (thickness of 0.2 cm; diameter of 3 to 5 cm) and stored at -80 °C until use. Initial moisture content of maca slices was 66%.

**Table 1—The levels of coded and uncoded values of independent variables.**

Symbol level/coded	1	0	−1
Freeze-thaw cycles	4	5	6
Thaw temperature (°C)	20	30	40
Ultrasonic time (min)	60	90	120

## Experiment design

**Optimization of pretreatments.** Maca root slices (3 replicates of 10 g each; 30 g total per pretreatment group) were tiled evenly in ziplock bags. Three replicates each were used for NP, FP, UP, and UFP, separately. For FP, the freeze-thaw cycles (1, 3, 6, or 9 cycles) were carried out alternately in a freezer (−20 °C) for 30 min and a water bath (20 °C) for 30 min. UP was performed in a thermostatic ultrasonic bath (KQ-400GKDV, Kunshan, China; 400 W, 40 KHz, 49 to 203 W/in<sup>2</sup>) at 20 °C and treated with 400 W for 3, 6, 9, or 12 hr. The ultrasonic power was set at 400 W based on the instrument parameter and our previous data (Figure S2A). For UFP, samples were alternate between a freezer (−20 °C) for freezing and a thermostatic ultrasonic bath for ultrasonic-assisted thawing. Conditions of UFP were optimized via single factor experiments and an orthogonal experimental design (Table 1). In single factor experiments, the common fixed conditions were thaw temperature: 30 °C, freeze-thaw cycles: 2, ultrasonic time: 20 min and freezing time: 2 hr. One chosen factor changed while other factors remained fixed. Conditions for FP, UP, and UFP were optimized according to the response values of benzylamine and free fatty acids based on fresh weight (FW). Macamide formation was also considered.

**Maca sample processing after pretreatment.** Maca root slices subjected to NP, FP, UP, and UFP were studied in comparison (Figure 2). After pretreatment, a portion (5 g) of each sample was ground into powder for the detection of benzylamine and free fatty acids. The remaining portion of each samples were applied to the drying study and LF-NMR. One part of dried slices was used for the studies of surface morphology and rehydration capacity. The other part was ground into powder for analyses of proximate composition and macamides.

## Drying studies

**Drying kinetics.** Maca slices (NP, FP, UP, and UFP) were dried at 30 °C as it is the best temperature for macamide formation (Figure S2B) (Chen et al., 2017). The weight of slices was measured every 30 min until the weight reduction was less than 0.1 g. The moisture ratio (*MR*) in samples was calculated using Eq. (1) on the basis of the simplified Fick's diffusion equation (Fijalkowska, Nowacka, Wiktor, Sledz, & Witrowa-Rajchert, 2016):

$$MR = \frac{M - M_e}{M_0 - M_e} \quad (1)$$

where *M* is the moisture content at any time; *M<sub>e</sub>* is the equilibrium moisture content and *M<sub>0</sub>* is the initial moisture content of maca samples.

Moreover, the effective moisture diffusivity (*D<sub>eff</sub>*) was calculated by Eq. (2) for maca samples.

$$MR = \frac{8}{\pi^2} \exp\left(-\frac{\pi^2 D_{eff} t}{4L^2}\right) \quad (2)$$

where *D<sub>eff</sub>* is the effective moisture diffusivity (m<sup>2</sup>/s); and *L* is the half thickness of maca slice (m).

**Low-field nuclear magnetic resonance (LF-NMR).** LF-NMR is a nondestructive, rapid and sensitive technique to monitor distributions of water components by measuring proton relaxation times (Sánchez-Alonso, Moreno, & Careche, 2014). Proton relaxation time constants includes longitudinal (*T<sub>1</sub>*) and transverse (*T<sub>2</sub>*). *T<sub>2</sub>* relaxometry can provide information on different water populations in the food matrixes. For the LF-NMR measurements, a NMI20-Analyst (Shanghai Niumag Corp., China) with a magnetic field strength of 0.5 Tesla, corresponding to a proton resonance frequency of 20 MHz was used. The magnet temperature was 32 °C to ensure the constant of the system. Samples, 0.2 cm × 1 cm × 2 cm portions of about 0.5 g were cut from the same part of the maca slices and placed in NMR tubes (15 mm in diameter). Transverse relaxation data (*T<sub>2</sub>*) were measured using the Carr–Purcell–Meiboom–Gill pulse sequence (CPMG). The parameters are set as follows: 8 scans, 12000 echoes, 5 s between scans, 90° pulse of 14 μs, 180° pulse of 28 μs, τ = 300 μs.

NMR *T<sub>2</sub>* transverse relaxation data was analyzed with the MultiExp Inv Analysis software (Niumag PQ001; SuzhouNiumag Analytical Instrument Corp., China), and was based on the inverse Laplace transform algorithm (Li et al., 2016).

## Physicochemical characteristics

**Scanning electron microscopy (SEM).** The morphological alterations of dried samples affected by NP, FP, UP, and UFP were observed on a JSM-6700F cold-field emission SEM (JEOL, Japan). The samples were fixed on a metal stub with a piece of conductive tape, and were coated with platinum under vacuum by a JFC-1600 ion sputter (JEOL, Japan).

**Rehydration capacity.** Rehydration experiments were carried out according to Maskan (2001) by immersing 1 g of dried slices into deionized water at 50 °C for 60 min. Every 10 min the samples were gently removed from the surface water with the paper towels and reweighed. The rehydration capacity was calculated as Eq. (3):

$$\text{weight gain(\%)} = \frac{(W_t - W_d)}{W_d} \times 100 \quad (3)$$

where *W<sub>t</sub>* is the weight of rehydrated samples (g) at the time of *t*, *W<sub>d</sub>* is the dry weight of samples (g).

**Proximate analyses.** Proximate compositions of NP, FP, UP, and UFP samples including moisture, ash, crude protein and fat contents were determined according to National Standard of China GB 5009.3, GB 5009.4, GB 5009.5, and GB 5009.6, respectively. The moisture content was determined by heating the samples at 105 °C until constant weight. The ash content was determined by incineration at 550 °C for 4 hr. The crude protein content (N × 6.25) was estimated by the Kjeldhal method (Kjeldahl 1983). The crude fat content was determined by a Soxhlet apparatus using petroleum ether as solvent. Total carbohydrate content was calculated by difference: 100 − (g ash + g protein + g crude fat) (Liu et al., 2012).

## Analysis of constituents involved in the biosynthesis of macamides

**Extraction and detection of benzylamine and free fatty acids.** The extraction method was according to Esparza et al. (2015) with slight modifications: after pretreatment, fresh maca slices were smashed with a pre-cooled pulverizer (Jouyong

**Table 2—Optimization of benzylamine and free fatty acids formation with orthogonal method.**

Run	Factors			Response	
	Freeze-thaw cycles (A)	Thaw temperature (°C) (B)	Ultrasonic time (min) (C)	Benzylamine (µg/g FW)	Free fatty acids (µg/g FW)
1	4	20	60	27.68	167.03
2	5	20	90	39.64	252.08
3	6	20	120	43.77	202.43
4	4	30	90	49.70	254.33
5	5	30	120	43.63	302.61
6	6	30	60	57.99	219.42
7	4	40	120	40.02	257.72
8	5	40	60	36.36	170.29
9	6	40	90	48.46	292.07

	Benzylamine (µg/g FW)			Free fatty acids (µg/g FW)		
	A	B	C	A	B	C
K1 <sup>a</sup>	39.13	37.03	40.67	226.36	207.18	185.58
K2	39.88	50.44	45.94	241.66	258.79	266.16
K3	50.07	41.62	42.47	237.97	240.03	254.25
R <sup>b</sup>	10.94	13.41	5.26	15.30	51.61	80.58

Important	B>A>C			C>B>A		
Order optimal level	A3	B2	C2	A2	B2	C2

<sup>a</sup>The  $k_i^A = \sum \text{Extraction yield at } A_i/3$ .

<sup>b</sup>The  $R_i^A = \sum \max(k_i^A) - \min(k_i^A)$ .

JYL-C010, China). A portion (5 g) was extracted in an ultrasonic bath with 100 mL 70% methanol under 200 W at 50 °C for 30 min. Samples were centrifuged at 5000 × g for 10 min. The supernatant was vacuum dried and redissolved in 5 mL with 70% methanol using a volumetric flask.

Benzylamine was analyzed by derivatization with dansyl chloride and detected by reversed phase HPLC. The 70% methanol extract (0.5 mL), 1 mg/mL dansyl chloride (C<sub>12</sub>H<sub>12</sub>ClNO<sub>2</sub>S) in acetonitrile (0.5 mL) and Na<sub>2</sub>CO<sub>3</sub>/NaHCO<sub>3</sub> (1 mL; pH 10.5) were mixed and placed in a water bath at 60 °C for 45 min. After cooling at room temperature for 10 min, ammonium hydroxide (NH<sub>3</sub>·H<sub>2</sub>O, 0.1 mL) was added and the solution was kept in the dark for 30 min. Twenty mg/mL methylamine hydrochloride (CH<sub>6</sub>ClN, 0.1 mL) was added, mixed and filtered through a 0.22 µm filter. HPLC analysis was carried out on an Agilent 1260 consisting of an autosampler and quaternary pump system (Agilent Technologies Co. Ltd., U.S.A.) coupled with a diode array detector. A 20 µL aliquot of each sample solution was injected and analyzed using a Megres C18 reversed-phase column (250 mm × 4.6 mm, 5 µm). The solvent system consisted of (A) sodium acetate buffer (pH 4.2, 10 mM) and (B) acetonitrile using an isocratic of 25:75 (A: B) for 10 min. The flow rate was set at 0.8 mL/min, and the column temperature was 30 °C. Chromatograms were recorded at 254 nm.

Samples were prepurified prior to free fatty acid determinations. Two milliliters of samples in 70% methanol were loaded onto a Poly-Sery HLB SPE column (60 mg, 3 mL). The column was washed with 50% methanol (2 mL) and eluted with methanol (1 mL). HPLC analysis was carried out using an Agilent 1260 with a Waters XTerra C18 (250 mm × 4.6 mm, 5 µm). The isocratic system consisted of (A) water containing 0.2% formic acid and (B) acetonitrile (10:90, v/v). The column temperature was 30 °C, flow at 0.6 mL/min, and elution was monitored at 210 nm.

**Extraction and detection of macamides.** Post-pretreatment maca slices were dried at 30 °C for 7 days, then ground

into powder and used for macamide analyses. Extraction and detection of macamides were according to our previous study [13]. One-gram of powder was extracted in an ultrasonic bath with 40 mL petroleum ether for 15 min at 200 W at 50 °C. After centrifugation, the supernatant was concentrated and brought to 5 mL with acetonitrile. The sample was filtered through a 0.22 µm filter before HPLC. HPLC-UV analysis was carried out on an Agilent 1260 with the following settings: column, reversed-phase C18; elution, acetonitrile: water: formic acid, 90:9.98:0.02; time, 35 min; flow rate, 0.6 mL/min; column temperature, 30 °C; detection wavelength, 210. The total content of macamides was calculated as the sum of *N*-benzyl-9Z, 12Z, 15Z-octadecatrienamide, *N*-benzyl-9Z, 12Z-octadecadienamide, and *N*-benzyl-hexadecanamide.

### Statistical analysis

Data are expressed as mean ± standard error using 3 replicates. All measurements were compared statistically by the IBM SPSS statistics software 19 (George & Mallery, 2011). Analyses of variance (ANOVA) were used to determine the differences among samples after different pretreatments at significance level  $P \leq 0.05$ .

## Results and Discussion

### Optimization of pretreatment conditions

Single factor experiments show that thawing at 40 °C, six freeze-thawing cycles with more than 2 hr of ultrasonic-assisted thaw time for each cycle are the best conditions for free fatty acid and benzylamine generation, while freeze time showed no effect (Figure S3). The formation of free fatty acids and benzylamine are important as they are the biosynthetic precursors of macamides. However, the conditions of pretreatment show critical impact on macamide formation. Therefore, the number of freeze-thaw cycles, thaw temperature and ultrasonic time for UFP were chosen as shown in Table 1 for the orthogonal (L<sub>9</sub>3<sup>4</sup>) test. The parameters were weighted and quantitatively analyzed using evaluation indices



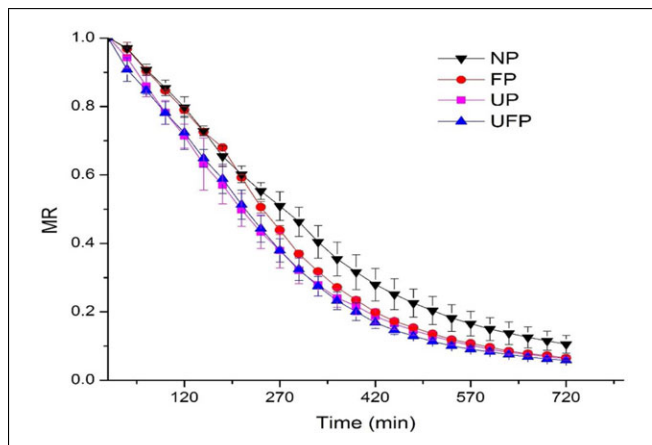


Figure 3—Drying curves of maca samples with different pretreatments.

$k$  and  $R$  (Table 2). The importance of selected factors for benzylamine formation were ranked as follows: thaw temperature > number of freeze-thaw cycles > ultrasonic time. The importance of selected factors for the formation of free fatty acids was ranked as follows: ultrasonic time > thaw temperature > number of freeze-thaw cycles. The optimal levels of the 3 factors needed to obtain the highest yield of benzylamine (A3B2C2) were minimally different from those needed to obtain the highest yield of free fatty acids (A2B2C2). Finally, the optimal conditions were found to be 90 min ultrasonic processing at 30 °C with six freeze-thaw cycles. For FP, the best conditions were found to be six cycles of freeze/thaw cycles (−20 °C/ 20 °C) each for 30 min. While the optimized conditions for UP were continuous treatment for 9 hr at 20 °C in the ultrasonic bath.

### Effect of pretreatments on drying characteristics

**Drying kinetics.** The drying curves (time vs MR) of 4 maca slices (NP, FP, UP, and UFP) are presented in Figure 3. The drying time required to reach a constant weight was determined to be 720 min. At present, the traditional open field drying is the most important method for maca drying, which usually takes about 90 d (Yábar et al., 2011). In this study, low-temperature oven drying (30 °C) significantly shortened the time to 720 min for maca drying. Similar decline trends in the MR were observed for all maca slices. NP sample exhibited a relatively slower drying rate and a higher equilibrium moisture content (8.19%) than FP (6.18%), UP (5.57%), and UFP (3.53%).

In order to reflect the drying rate more precisely, the values of effective moisture diffusivity were calculated further and listed in Table 3. The sample of UFP had the highest  $D_{eff}$  value of  $1.75 \times 10^{-9} \text{ m}^2/\text{s}$ , followed by UP of  $1.70 \times 10^{-9} \text{ m}^2/\text{s}$ , FP of  $1.68 \times 10^{-9} \text{ m}^2/\text{s}$  and NP of  $1.37 \times 10^{-9} \text{ m}^2/\text{s}$ . The results indicated that both UP and FP increased the drying efficiency. When the effects of ultrasound and freeze-thawing were combined for the UFP, the drying efficiency was strengthened. These results might be due to a change in the tissue structure of the maca slices affected by different pretreatments.

Tatemoto, Mibu, Yokoi, and Hagimoto (2016) found that a higher drying rate was achieved for carrots using freezing pretreatment. Ando et al. (2016) reported that carrot roots pretreated with freeze-thaw cycles showed the highest drying rate. Chen, Guo, and Wu (2016) studied a novel ultrasound and vacuum drying method and found that this method decreased the drying time by 41% to 53%. In this study, no significant reduction in drying

Table 3—Effective diffusivity values of NP, FP, UP, and UFP samples.

Samples	Drying time (min)	$D_{eff} \times 10^9 \text{ (m}^2/\text{s)}$
NP	720	$1.37 \pm 0.18^a$
FP	720	$1.68 \pm 0.02^b$
UP	720	$1.70 \pm 0.06^b$
UFP	720	$1.75 \pm 0.05^b$

Mean followed by different letters in the same column differs significantly ( $P \leq 0.05$ ).

time was found in pretreatment samples. We hypothesize this phenomenon might be the result of the samples not being immersed directly in water and the ultrasound was applied through a ziplock bag, which weakened the actual power of ultrasound. Nowacka and Wedzik (2016) reported that no time reduction was observed in ultrasound-treated carrot tissue when compared with untreated samples. The samples were vacuum-packed and treated with ultrasounds using 21 and 35 kHz frequency for 10, 20, and 30 min. This phenomenon might be due to the packaging of samples.

**Proton LF-NMR relaxation analysis.** LF-NMR has been widely accepted as a powerful technique for the characterization of water mobility and distribution in food (Li et al, 2014). Figure 4; Ribeiro et al., 2014 shows the distributed  $T_2$  relaxation-time spectra of 4 maca samples at 0, 360, or 720 min of the drying process.  $T_2$  relaxation time reflects the degree of freedom of water and the relative amplitude of relaxation relates to water content (Li et al., 2016). The  $T_2$  decay curve is a visual reflection of drying kinetics of samples and it also can provide information on tissue morphology (Sánchez-Alonso et al., 2014).

As shown in Figure 4A to C, two bands were found in NP, FP and UP samples at the drying time of 0 min (black line). A small band ( $T_{21}$ ) centered at 4 to 6 ms, accounting for 5% to 7% of the total signal and a major band ( $T_{22}$ ) centered at 40 to 65 ms accounting for 92% to 95% of the total signal. Similar distributed  $T_2$  relaxation times were observed in potato and broccoli tissues (Straadt, Thybo, & Bertram, 2008; Xin, Zhang, & Adhikari, 2013). It was reported that  $T_{21}$  represents the less mobile water residing in the cytoplasm and  $T_{22}$  is assigned to the more mobile water located within the vacuole. In Figure 4D, the distribution of  $T_2$  relaxation data in UFP sample shows three population groups of protons:  $T_{21}$  centered at 3.6 ms accounting for 5.7% of the total signal,  $T_{22}$  centered at 27 ms accounting for 87.7% of the total signal and  $T_{2a}$  which adhered to  $T_{22}$ , centered at 113.5 ms accounting for 6.4% of the total signal. These results showed that UFP changed the state of water in maca slices. Xu, Zhang, Bhandari, Cheng, and Sun (2015) reported that ultrasound-assisted immersion freezing would enhance the water mobility by decreasing the vacuole water and increasing cytoplasm and intercellular space water. In this study, UFP significantly affected the mobility and distribution of water in maca slices while ultrasound or freeze-thaw treatments showed no significant effect.

The drying kinetics of maca samples also can be reflected by the  $T_2$  transverse relaxation time distribution. According to the black, red and blue lines in Figure 4, the signal of water contained in maca samples changed gradually as the drying proceeded. The  $T_2$  relaxation time decreased with the extension of the drying time, suggesting that water mobility declined which might be due to a more compact cell structure. Moreover, it was clear that the amplitude of  $T_2$  decreased remarkably with extension of drying time because of reduced water content. The consistent variation trend in water detected by LF-NMR during the drying process

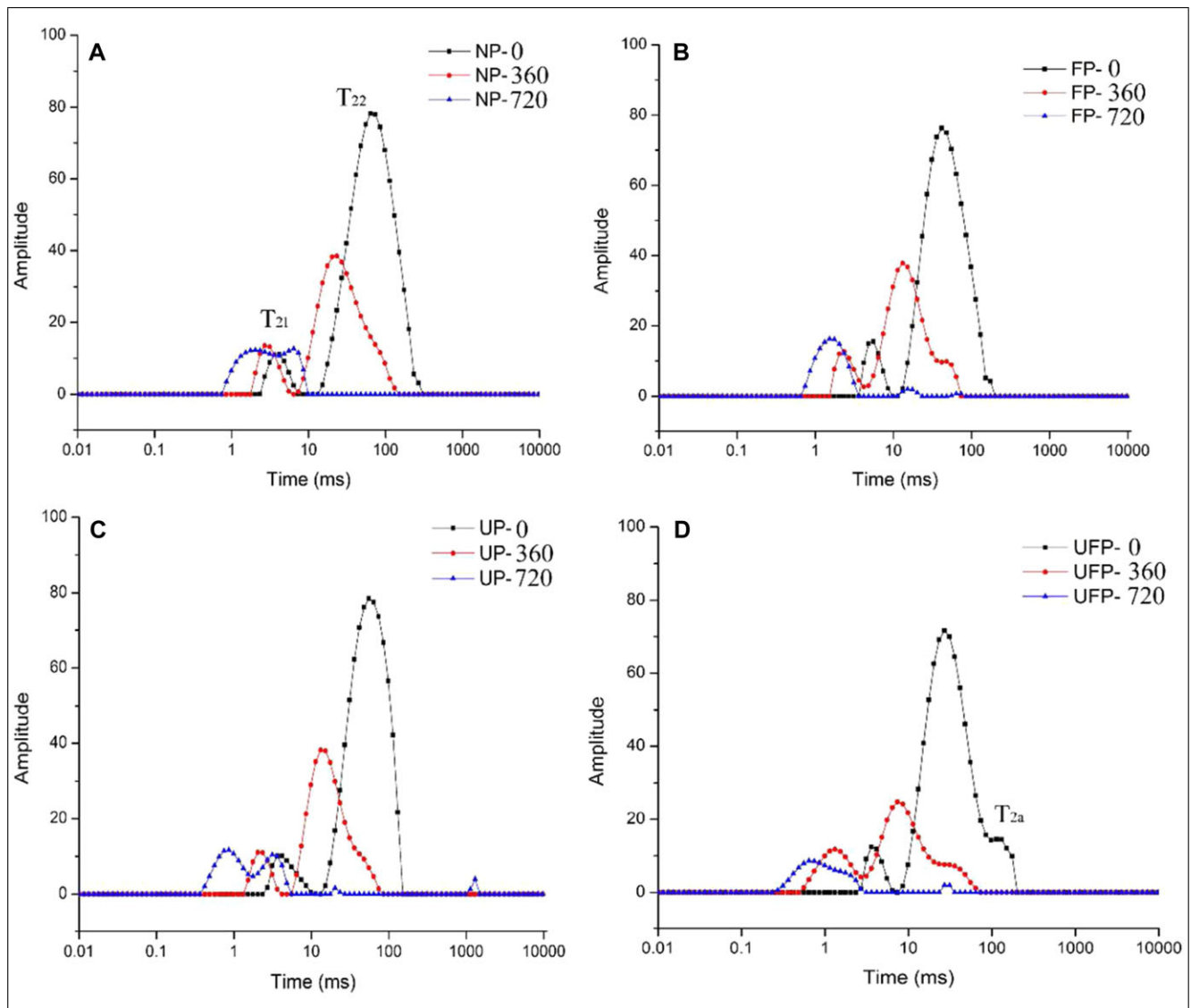


Figure 4—LF-NMR T<sub>2</sub> distribution of maca samples at the drying time of 0 min (black line, -0), 360 min (red line, -360) and 720 min (blue line, -720). (A) NP; (B) FP; (C) UP; (D) UFP. For the black and red line, the first bond was T<sub>21</sub> and the second bond was T<sub>22</sub>, in black and red line, while the small peak adhered to T<sub>22</sub> in Figure 4D was T<sub>2a</sub>.

was also observed in chicken jerky and apple (Li et al., 2014; Mothibe, Zhang, Mujumdar, Wang, & Cheng, 2014).

### Effect of pretreatments on surface morphology

The SEM photos of dried maca subjected to different pretreatments showed a remarkable difference in the microstructure of maca slices. As shown in Figure 5A, cells are densely arranged, and the surface is smooth and compacted on the surface of the NP sample. Large numbers of oval granules (5 to 10  $\mu\text{m}$  diameter) were observed and were previously reported as starch granules (Chen et al., 2015). For the FP sample (Figure 5B), cracks and very small cavities were observable on the surfaces. Compared with NP and FP samples, UP and UFP samples showed more irregular surfaces with cracks and large cavities (Figure 5C and D). The microscopic image indicated that both ultrasound and FP used before drying caused structural damage and cell breakdown of the materials. Previous studies reported the effects of ultrasound on cell damage and microchannel creation (Chen et al., 2016; Nowacka & Wedzik, 2016). Large spaces in cell walls due to the formation of ice crys-

tals created by FP (Ando et al., 2016). In this study, we found an enhanced destructive effect on microstructure with combination of ultrasound and freeze-thaw cycles.

**Effect of pretreatments on rehydration.** Rehydration capacity of a dried product is used as an evaluation index for decent quality. The rehydration curves of 4 maca samples are shown in Figure 6. The amount of moisture absorbed increases with rehydration time in all samples, but at a decreasing rate up to saturation level. The NP sample showed the fastest rehydration in 10 min and the rehydration stabilized in about 30 min for NP and UP, and about 50 min for FP and UFP. The final rehydration ratios of NP, FP, UP, and UFP acquired under the same drying conditions were 1.26, 1.32, 1.46, and 1.61, respectively. The FP, UP, and UFP samples showed higher moisture contents than NP after rehydration. It might be because of more porous structures in the plant matrix caused by pretreatments. For this experimental condition, the rehydration of NP, FP, and UP samples did not reach a moisture content higher than 1.5 (water content of original sample is 66%, which is 1.94). These phenomena can be attributed

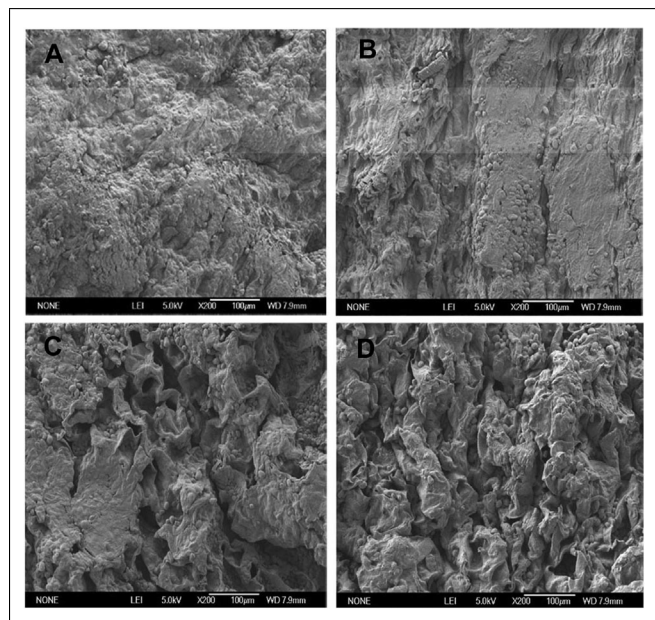


Figure 5—Scanning electron micrographs of dried maca slices. (A) NP; (B) FP; (C) UP; (D) UFP.

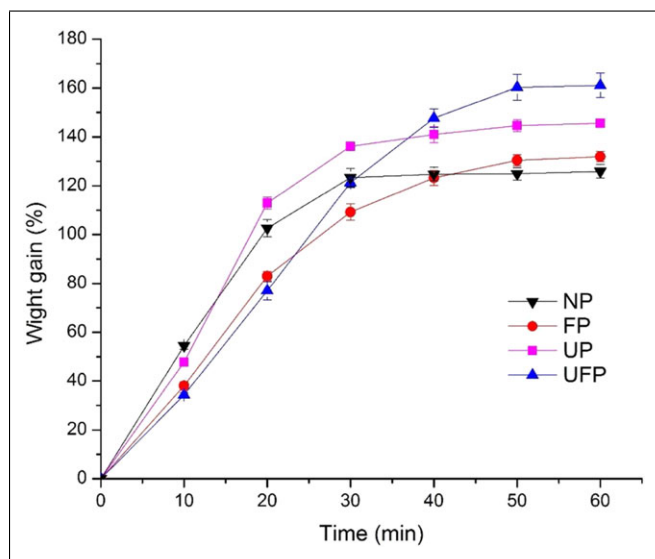


Figure 6—Rehydration curves of dried maca slices.

to structural damage and cell shrinkage caused by pretreatment, which resulted in the loss of rehydration ability. Jambak et al. (2007) deemed that the dehydration procedure is irreversible as they found the equilibrium moisture content of rehydrated samples could not reach the moisture content of raw materials.

**Effect of pretreatments on proximate composition.** The chemical compositions of maca samples are shown in Table 4. A

similar composition of maca had been reported by Dini, Migliuolo, Rastrelli, Saturnino, and Schettino (1994). Compared with NP sample (8.19%), lower contents of moisture were found in FP (6.18%), UP (5.57%), and UFP (3.53%), and were attributed to the changes in water state and microstructure mentioned above. As to the content of macronutrients, statistically significant differences were found between treated samples and NP control for ash, protein and carbohydrates but not for crude lipid. It was interesting that pretreatment reduced the content of ash and carbohydrates but increased the content of crude protein. Few studies have been reported in this area. Further research is needed to illustrate the underlying mechanism.

### Effect of pretreatments on biosynthesis of macamides

#### Formation of benzylamine and free fatty acids in fresh slices.

The concentrations of benzylamine and free fatty acids in fresh maca slices affected by different pretreatments are shown in Figure 7A. NP sample only contained 4.32  $\mu\text{g/g}$  of benzylamine and 29.92  $\mu\text{g/g}$  of free fatty acids. Both contents were significantly increased to 29.83 and 97.04  $\mu\text{g/g}$  by FP and to 58.23 and 125.93  $\mu\text{g/g}$  by UP, respectively. Under the optimized UFP condition, the productions of benzylamine and free fatty acids increased to 54.33 and 259.13  $\mu\text{g/g}$ , respectively, which are almost 10-fold as those of untreated sample.

Glucosinolate and myrosinase are in different compartments in intact cells (Thangstad, Bones, Holtan, Moen, & Rossiter, 2001). Yábar et al. (2011) and Esparza et al. (2015) reported that the natural freeze-thaw cycles were beneficial to the contact between glucosinolate and myrosinase to enhance the formation of benzylamine. Moreover, the natural freeze-thaw cycles also lead to the release of free fatty acids from storage and membrane lipids by tissue maceration. This study showed that freeze-thaw cycles in the laboratory had similar positive effects on benzylamine and free fatty acid formation. More than that, better effects were observed in the sample treated with ultrasound. Ultrasound has been reported to enhance various important bio-processes, such as fermentations, enzymatic transformations, food processing and enzyme assisted chemical synthesis (Sutar & Rathod, 2015; Waghmare & Rathod, 2016). Marchesini et al. (2012) found that ultrasound treatment of milk significantly increased the free fatty acid levels. Ultrasound treatment appears to make lipid micelles more accessible to lipases. However, continuous ultrasound treatment may lead to deactivation of the enzyme and damage to the ultrasonic transducers. In this study, ultrasound was used in periodic manner combined with freeze-thaw cycles. As a result, the concentrations of benzylamine and free fatty acids are highly enhanced in a relatively short time.

Esparza et al. (2015) detected 40.2  $\mu\text{mol/g}$  of benzylamine and 4.3  $\mu\text{mol/g}$  of free fatty acids in maca root. The samples were exposed to high irradiance, low humidity and extremes of temperature, and treated with a combination of mechanical damage, freeze-thaw cycles and dehydration of tissues for 77 days. Relatively low contents of benzylamine and free fatty acids were found

Table 4—Moisture (% of FW) and macronutrients (% of DW) of dried NP, FP, UP, and UFP samples.

Samples	Moisture	Ash	Crude protein	Crude lipid	Carbohydrates
NP	8.19 ± 2.19 <sup>ab</sup>	3.63 ± 0.07 <sup>a</sup>	13.69 ± 0.13 <sup>a</sup>	2.23 ± 0.30 <sup>a</sup>	80.45 ± 0.39 <sup>ab</sup>
FP	6.18 ± 1.41 <sup>b</sup>	2.94 ± 0.02 <sup>b</sup>	15.99 ± 0.39 <sup>b</sup>	2.32 ± 0.14 <sup>a</sup>	78.75 ± 0.46 <sup>b</sup>
UP	5.57 ± 1.15 <sup>b</sup>	3.16 ± 0.06 <sup>c</sup>	15.42 ± 0.12 <sup>b</sup>	2.63 ± 0.31 <sup>a</sup>	78.79 ± 0.33 <sup>b</sup>
UFP	3.53 ± 0.81 <sup>bc</sup>	3.39 ± 0.06 <sup>d</sup>	16.29 ± 0.56 <sup>b</sup>	2.30 ± 0.34 <sup>a</sup>	78.02 ± 0.77 <sup>bc</sup>

Mean followed by different letters in the same column differs significantly ( $P \leq 0.05$ ).

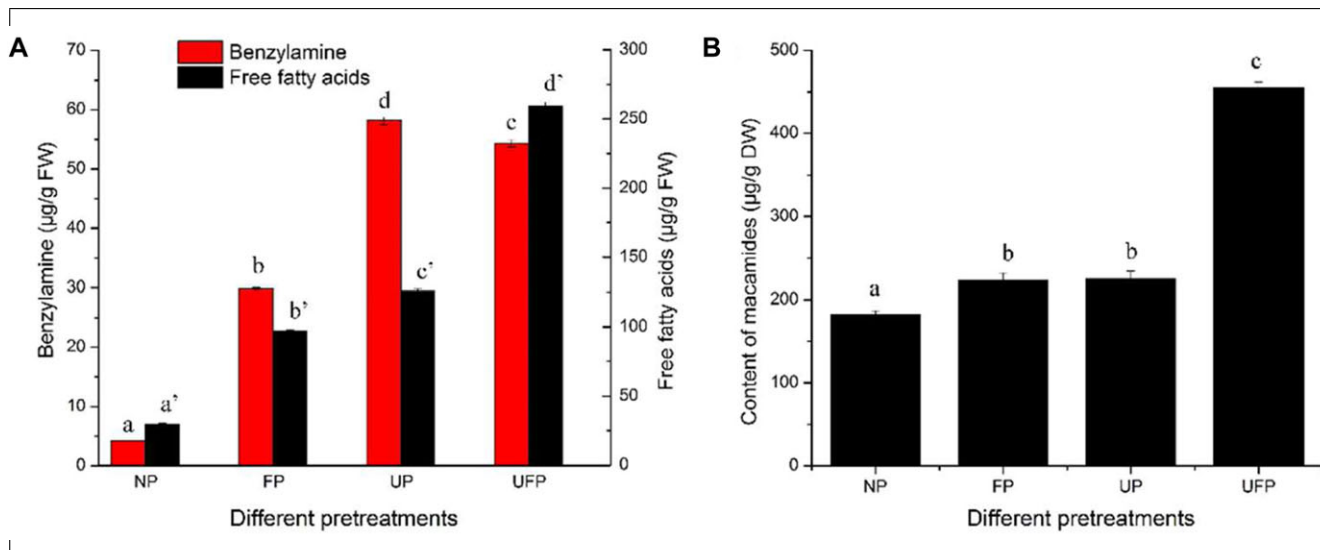


Figure 7—Contents of benzylamine and free fatty acids in fresh maca (A) and contents of macamides in dried maca (B) affected by different pretreatments. Bars with different letters indicate statistical difference ( $P \leq 0.05$ ).

in this study might be due to the following reasons: first, the contents of benzylamine and free fatty acids were calculated based on fresh weight; second, maca samples were treated less extreme and for a short time. However, the experimental conditions are more convenient for maca industrial application.

**Formation of macamides in dried slices.** We further examined macamide contents in those maca samples. The chromatograms of macamide standards and maca samples were shown in Figure 4S. The contents of macamides were shown in Table S1 and Figure 7. Statistically significant differences were found among pretreated samples when compared to the untreated sample. NP sample has the lowest content of macamides ( $182.11 \mu\text{g/g}$ ). Samples of FP and UP contained similar amounts of macamides,  $222.90$  and  $225.04 \mu\text{g/g}$ , respectively. The UFP sample showed the highest content of macamides ( $455.45 \mu\text{g/g}$ ), which is about 2.5-fold of that in the NP sample. The non-corresponding proportional relationship between contents of macamides and their precursors indicated that the formation of the amide bonds between benzylamine and free fatty acids is a critical rate-limiting step in macamide formation. Esparza et al. (2015) speculated that the amide bond formation might be catalyzed by a fatty acid amide hydrolase (FAAH) working in reverse. Nonribosomal peptide synthetases (Strieker, Tanović, & Marahiel, 2010) or bifunctional peptidylglycine  $\alpha$ -amidating enzyme ( $\alpha$ -AE) (Wilcox et al., 1999) could also be involved in macamide biosynthesis. However, considerable efforts are still needed to unravel the biochemical origin of these moieties.

## Conclusions

A novel method of UFP was designed and optimized for fresh maca process in this study. Compared with samples with NP, FP, and UP, UFP sample showed a higher drying efficiency because of changes of the internal water state and microstructure of maca slices. The rehydration and protein content of maca were also improved by UFP. More importantly, UFP increased macamide accumulation 2.5-fold and its biosynthetic precursor formation 10-fold, respectively, in a short time, when compared with the untreated sample. These results suggest that appropriate pretreatment for fresh maca would improve the quality and chemical composition of derived commercial maca products. However, en-

ergy consumption for this process is important in the industrial manufacture of maca products. It is impractical to calculate the energy consumption in this study due to equipments used. Therefore, we have an ultrasound-assisted freeze-thaw drying equipment specially designed for this task (Figure S5). Further research on energy requirements for this process can be carried out in the future using this setup.

## Acknowledgment

This work was supported by the National Natural Science Fund of China (No. 21506220).

## Conflict of interest

The authors declare that they have no competing interests.

## References

- Almukadi, H., Wu, H., Böhlke, M., Kelley, C. J., Maher, T. J., & Pino-Figueroa, A. (2013). The macamide N-3-methoxybenzyl-linoleamide is a time-dependent fatty acid amide hydrolase (FAAH) inhibitor. *Molecular Neurobiology*, *48*(2), 333–339.
- Alquraini, A., Waggas, D., Böhlke, M., Maher, T., & Pino-Figueroa, A. (2014). Neuroprotective effects of *Lepidium meyenii* (Maca) and macamides against amyloid-beta (25–35) induced toxicity in B-35 neuroblastoma cells. *The FASEB Journal*, *28*(1), Supplement 657.13.
- Ando, Y., Maeda, Y., Mizutani, K., Wakatsuki, N., Hagiwara, S., & Nabetani, H. (2016). Impact of blanching and freeze-thaw pretreatment on drying rate of carrot roots in relation to changes in cell membrane function and cell wall structure. *LWT - Food Science and Technology*, *71*, 40–46.
- Bones, A. M., & Rossiter, J. T. (1996). The myrosinase-glucosinolate system, its organisation and biochemistry. *Physiologia Plantarum*, *97*(1), 194–208.
- Chemat, F., & Khan, M. K. (2011). Applications of ultrasound in food technology: Processing, preservation and extraction. *Ultrasonics Sonochemistry*, *18*(4), 813–835.
- Chen, J., Zhao, Q., Liu, Y., Gong, P., Cao, L., Wang, X., & Zhao, B. (2017). Macamides present in the commercial maca (*Lepidium meyenii*) products and the macamide biosynthesis affected by postharvest conditions. *International Journal of Food Properties*, *20*(12), 3112–3123.
- Chen, J., Zhao, Q., Wang, L., Zha, S., Zhang, L., & Zhao, B. (2015). Physicochemical and functional properties of dietary fiber from maca (*Lepidium meyenii* Walp.) liquor residue. *Carbohydrate Polymers*, 509–512.
- Chen, Z.-G., Guo, X.-Y., & Wu, T. (2016). A novel dehydration technique for carrot slices implementing ultrasound and vacuum drying methods. *Ultrason. Sonochem.*, *30*, 28–34.
- Dini, A., Migliuolo, G., Rastrelli, L., Saturnino, P., & Schettino, O. (1994). Chemical composition of *Lepidium meyenii*. *Food Chemistry*, *49*(4), 347–349.
- Dussert, S., Davey, M., Laffargue, A., Doulebeau, S., Swennen, R., & Etienne, H. (2006). Oxidative stress, phospholipid loss and lipid hydrolysis during drying and storage of intermediate seeds. *Physiologia Plantarum*, *127*(2), 192–204.
- Esparza, E., Hadzich, A., Kofer, W., Mithöfer, A., & Cosio, E. G. (2015). Bioactive maca (*Lepidium meyenii*) alkaloids are a result of traditional Andean postharvest drying practices. *Phytochemistry*, *116*, 138–148.
- Fijalkowska, A., Nowacka, M., Wiktor, A., Sledz, M., & Witrowa-Rajchert, D. (2016). Ultrasound as a pretreatment method to improve drying kinetics and sensory properties of dried apple. *Journal of Food Process Engineering*, *39*(3), 256–265.



- George, D., & Mallery, P. (2011). *IBM SPSS statistics 19 step by step: A simple guide and reference* (13th ed.). Pearson Higher Ed.
- Gonzales, G. F. (2012). Ethnobiology and ethnopharmacology of *Lepidium meyenii* (Maca), a plant from the Peruvian highlands. *Evidence-Based Complementary and Alternative Medicine*, 2012, 1–10.
- Hajdu, Z., Nicolussi, S., Rau, M., Lorántfy, L.s., Forgo, P., Hohmann, J., ... Gertsch, J.r. (2014). Identification of endocannabinoid system-modulating N-alkylamides from *Heliposid helianthoides* var. *scabra* and *Lepidium meyenii*. *Journal of Natural Products*, 77(7), 1663–1669.
- Jambrak, A. R., Mason, T. J., Paniwnyk, L., & Lelas, V. (2007). Accelerated drying of button mushrooms, Brussels sprouts and cauliflower by applying power ultrasound and its rehydration properties. *Journal of Food Engineering*, 81(1), 88–97.
- Kjeldahl, J. (1983). A new method for the determination of nitrogen in organic matter. *Journal of Analytical Chemistry*, 22(1), 366–382.
- Lewis, S., & Pino-Figueroa, A. (2013). Neuroprotective effects of Maca extract and macamides against amyloid  $\beta$ ; peptide induced neurotoxicity in B-35 neuroblastoma cells. *The FASEB Journal*, 27, 662.19.
- Li, M., Wang, H., Zhao, G., Qiao, M., Li, M., Sun, L., ... Zhang, J. (2014). Determining the drying degree and quality of chicken jerky by LF-NMR. *Journal of Food Engineering*, 139, 43–49.
- Li, Y., Li, X., Chen, C., Zhao, D., Su, Z., Ma, G., & Yu, R. (2016). A rapid, non-invasive and non-destructive method for studying swelling behavior and microstructure variations of hydrogels. *Carbohydrate Polymers*, 151, 1251–1260.
- Liu, H., Jin, W., Fu, C., Dai, P., Yu, Y., Huo, Q., & Yu, L. (2015). Discovering anti-osteoporosis constituents of maca (*Lepidium meyenii*) by combined virtual screening and activity verification. *Food Research International*, 77, 215–220.
- Liu, Y., Sun, J., Luo, Z., Rao, S., Su, Y., Xu, R., & Yang, Y. (2012). Chemical composition of five wild edible mushrooms collected from Southwest China and their antihyperglycemic and antioxidant activity. *Food and Chemical Toxicology*, 50(5), 1238–1244.
- Marchesini, G., Balzan, S., Montemurro, F., Fasolato, L., Andrighetto, I., Segato, S., & Novelli, E. (2012). Effect of ultrasound alone or ultrasound coupled with CO<sub>2</sub> on the chemical composition, cheese-making properties and sensory traits of raw milk. *Innovative Food Science & Emerging Technologies*, 16, 391–397.
- Maskan, M. (2001). Drying, shrinkage and rehydration characteristics of kiwifruits during hot air and microwave drying. *Journal of Food Engineering*, 48(2), 177–182.
- Mothibe, K. J., Zhang, M., Mujumdar, A. S., Wang, Y. C., & Cheng, X. (2014). Effects of ultrasound and microwave pretreatments of apple before spouted bed drying on rate of dehydration and physical properties. *Drying Technology*, 32(15), 1848–1856.
- Nowacka, M., & Wedzik, M. (2016). Effect of ultrasound treatment on microstructure, colour and carotenoid content in fresh and dried carrot tissue. *Applied Acoustics*, 103, 163–171.
- Pan, Y., Zhang, J., Li, H., Wang, Y.-Z., & Li, W.-Y. (2016). Simultaneous analysis of macamides in Maca (*Lepidium meyenii*) with different drying process by liquid chromatography tandem mass spectrometry. *Food Analytical Methods*, 9(6), 1686–1695.
- Ribeiro, R. D. O.R., Mársico, E. T., da Silva Carneiro, C., Monteiro, M. L. G., Júnior, C. C., & de Jesus, E. F. O. (2014). Detection of honey adulteration of high fructose corn syrup by low field nuclear magnetic resonance (LF 1 H NMR). *Journal of Food Engineering*, 135, 39–43.
- Sánchez-Alonso, I., Moreno, P., & Careche, M. (2014). Low field nuclear magnetic resonance (LF-NMR) relaxometry in hake (*Merluccius merluccius* L.) muscle after different freezing and storage conditions. *Food Chemistry*, 153, 250–257.
- Straadt, I. K., Thybo, A. K., & Bertram, H. C. (2008). NaCl-induced changes in structure and water mobility in potato tissue as determined by CLSM and LF-NMR. *LWT - Food Science and Technology*, 41(8), 1493–1500.
- Strieker, M., Tanović, A., & Marahiel, M. A. (2010). Nonribosomal peptide synthetases: Structures and dynamics. *Current Opinion in Structural Biology*, 20(2), 234–240.
- Sutar, R. S., & Rathod, V. K. (2015). Ultrasound assisted enzyme catalyzed degradation of Cetirizine dihydrochloride. *Ultrasonics Sonochemistry*, 24, 80–86.
- Tatemoto, Y., Mibu, T., Yokoi, Y., & Hagimoto, A. (2016). Effect of freezing pretreatment on the drying characteristics and volume change of carrots immersed in a fluidized bed of inert particles under reduced pressure. *Journal of Food Engineering*, 173, 150–157.
- Thangstad, O. P., Bones, A. M., Holtan, S., Moen, L., & Rossiter, J. T. (2001). Microautoradiographic localisation of a glucosinolate precursor to specific cells in *Brassica napus* L. embryos indicates a separate transport pathway into myrosin cells. *Planta*, 213(2), 207–213.
- Vaccarezza, L. M., Lombardi, J. L., & Chirife, J. (1974). Kinetics of moisture movement during air drying of sugar beet root. *International Journal of Food Science & Technology*, 9(3), 317–327.
- Waghmare, G. V., & Rathod, V. K. (2016). Ultrasound assisted enzyme catalyzed hydrolysis of waste cooking oil under solvent free condition. *Ultrasonics Sonochemistry*, 32, 60–67.
- Wilcox, B. J., Ritenour-Rodgers, K. J., Asser, A. S., Baumgart, L. E., Baumgart, M. A., Boger, D. L., ... Henz, M. E. (1999). N-Acylglycine amidation: Implications for the biosynthesis of fatty acid primary amides. *Biochemistry*, 38(11), 3235–3245.
- Wu, H., Kelley, C. J., Pino-Figueroa, A., Vu, H. D., & Maher, T. J. (2013). Macamides and their synthetic analogs: Evaluation of in vitro FAAH inhibition. *Bioorganic & Medicinal Chemistry*, 21(17), 5188–5197.
- Xin, Y., Zhang, M., & Adhikari, B. (2013). Effect of trehalose and ultrasound-assisted osmotic dehydration on the state of water and glass transition temperature of broccoli (*Brassica oleracea* L. var. botrytis L.). *Journal of Food Engineering*, 119(3), 640–647.
- Xu, B.-G., Zhang, M., Bhandari, B., Cheng, X.-F., & Sun, J. (2015). Effect of ultrasound immersion freezing on the quality attributes and water distributions of wrapped red radish. *Food and Bioprocess Technology*, 8(6), 1366–1376.
- Yábar, E., Pedreschi, R., Chirinos, R., & Campos, D. (2011). Glucosinolate content and myrosinase activity evolution in three maca (*Lepidium meyenii* Wálp.) ecotypes during preharvest, harvest and postharvest drying. *Food Chemistry*, 127(4), 1576–1583.
- Zhang, M., & Willison, J. (1992). Electrical impedance analysis in plant tissues: The effect of freeze-thaw injury on the electrical properties of potato tuber and carrot root tissues. *Canadian Journal of Plant Science*, 72(2), 545–553.

## Supporting Information

Additional Supporting Information may be found in the online version of this article at the publisher's website:

**Figure S1.** chemical structures of benzylamine, free fatty acids and macamides.

**Figure S2.** Effects of ultrasonic power (A) and temperature (B) on macamide fomatation during the drying process.

**Figure S3.** Effects of different factors in pretreatment process (A: UFP, B: FP, C: UP) on the generation of benzylamine, free fatty acids and macamides.

**Figure S4.** Chromatogram of macamide standards (A), chromatogram of four maca samples (B) and their 3D signal overlay (C) M1 is N-benzyl-9Z, 12Z, 15Z-octadecatrienamamide, M2 is N-benzyl-9Z, 12Z-octadecadienamamide and M3 is N-benzyl-hexadecanamamide.

**Figure S5.** Ultrasound-assisted freeze-thaw drying (UFD) equipment.

**Table S1.** Macamide contents in four maca samples after pretreatments.